Carrier thermalization in Cu_2O: Phonon emission by excitons

D. W. Snoke, D. Braun, and M. Cardona
Max-Planck-Institut für Festkörperforschung, Heisenbergstrasse 1, 7000 Stuttgart 80, Germany
(Received 4 March 1991)

We have observed the energy distribution of nonthermalized excitons in the semiconductor Cu_2O on a time scale of 10 ps following resonant creation by a short (5-ps) laser pulse. We present a model for the change in the energy distribution of carriers as they cool to take on a Maxwell-Boltzmann distribution at the lattice temperature. Emission and absorption of acoustic phonons via the deformation-potential interaction and emission and absorption of nonpolar optical phonons are taken into account in an exact Boltzmann equation that is solved numerically. The model fits the observed distributions well, for a value of the deformation potential in agreement with hydrostatic-pressure and uniaxial-stress measurements. Single-optical-phonon emission is found to be rather slow, with a time scale of about 30 ps. We also present evidence for a fast two-optical-phonon emission process in Cu_2O. Finally, we consider the effects of exciton-exciton interactions and obtain an upper bound on the range of exciton-exciton interactions from these experiments.

I. INTRODUCTION

With the development of short-laser-pulse generation and optical detection methods with time scales of picoseconds or less, the possibility exists for observing electronic processes in which the carriers are far from equilibrium, with neither a Maxwell-Boltzmann nor a Fermi-Dirac energy distribution, so that no temperature can be defined. The semiconductor Cu_2O presents an ideal opportunity for the study of such behavior in intrinsic, free excitons.[1] Because the binding energy of the excitons is high (150 meV), very few free carriers exist during excitation at low temperature. The high binding energy corresponds to a small excitonic Bohr radius (7 Å), which means that the excitons retain their identity up to high densities without a Mott transition. Because Cu_2O is a direct-band-gap semiconductor with nondegenerate conduction and valence bands, no electron-hole liquid phase exists. Unlike most direct-gap semiconductors, however, Cu_2O has long excitonic lifetimes (10 μs) because direct recombination is dipole forbidden.[2] In addition, extremely high-purity natural samples are available, with measured excitonic mean free path of 70 μm at low temperature[3] and a full width at half maximum (FWHM) of the direct-recombination luminescence line equal to only 0.03 meV at low temperature.

Study of the thermalization of excitons in Cu_2O is made possible by the fact that a relatively bright phonon-assisted recombination luminescence line appears. Because the matrix element of the optical-phonon-assisted recombination process is independent of the excitonic energy, the intensity of luminescence at photon energy $E_{\text{gap}}-E_{\text{binding}}-E_{\text{phonon}}+E_k$ is simply proportional to the number of excitons with kinetic energy E_k. Here the band-gap energy E_{gap}, the excitonic binding energy E_{binding}, and the optical-phonon zone-center energy E_{phonon} are all constants. The shape of the phonon-assisted line therefore gives the kinetic-energy distribution of the excitons directly.

This property has been used for the observation of Bose-Einstein statistical effects in Cu_2O.[4–9] These results include the recent observation of the narrowing of the FWHM of the exciton energy distribution to below the FWHM of the excitonic Maxwell-Boltzmann energy distribution at the crystal lattice temperature,[9] previously seen only in Ge under stress,[10] and the observation of sharp features ($dE \ll kT$) in the energy distribution of the excitons in quasi-steady at high excitonic density.[6,7]

In these works on Cu_2O, a fairly high increase in quasi-steady-state excitonic temperature was observed with increasing exciton density, dubbed "Bose-Einstein saturation"[5] because the temperature remains a constant fraction above the critical temperature for Bose-Einstein condensation over a large range of density. The rise in observed excitonic temperature does not occur because of lattice temperature increase or excitonic lifetime shortening.[8] One possible source of this heating is a four-particle (two-exciton) Auger nonradiative recombination/ionization process;[11,12] another possibility is the quantum-mechanical increase in kinetic energy due to confinement of the excitons by exciton-exciton interactions.[13] Before accurate modeling of the temperature rise can occur, however, the phonon emission rates and exciton-exciton scattering cross section must be known.

In addition to this motivation, study of the excitonic thermalization processes in Cu_2O is motivated by the observations of the thermalization of free carriers in semiconductors, such as seen in GaAs.[14] Although the carrier population of GaAs in general includes both free carriers and excitons, only the free carrier energy distribution can be deduced by luminescence line-shape analysis.

In this paper we report the observation of the energy distribution of excitons in Cu_2O resolved on time scales

of 10 ps after generation by laser pulses of 5–7-ps duration in the range 2.03–2.10 eV. The excitation conditions fall into two categories: (1) generation followed by relaxation by acoustic phonon emission and (2) generation followed by both optical phonon and acoustic phonon emission. We find that the energy distribution of the excitons during thermalization by acoustic phonon emission can be well fit at all times by a numerical model which assumes acoustic phonon emission for carriers via a deformation-potential interaction, and we obtain a value for an effective excitonic deformation potential. This effective deformation potential can be related to the shift in exciton energy observed in hydrostatic-pressure and uniaxial-stress measurements, and we find that the effective deformation potential we measure here is in agreement with these experiments. We also obtain a value for the deformation potential of the optical-phonon emission process assuming nonpolar optical-phonon emission. The emission times for single optical phonons in Cu_2O turn out to be rather slow, about 30 ps, compared to 180 fs for polar optical-phonon emission in GaAs. A two-optical-phonon emission process in Cu_2O, which does not have the symmetry constraints of the one-phonon emission process, occurs at a rate more than an order of magnitude faster.

In Sec. IV of this paper we discuss the effects of exciton-exciton scattering on the thermalization of the excitons. From our observations we obtain an upper limit for the exciton-exciton scattering cross section.

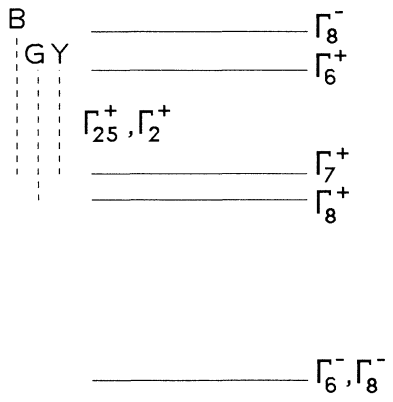

FIG. 1. Level diagram of the bands of Cu_2O at $\mathbf{k}=0$. The energy spacings of the levels are not drawn to scale. The "yellow" (Y) exciton series is formed from the Γ_6^+ conduction band and Γ_7^+ valence band and splits into the Γ_{25}^+ "orthoexciton" and Γ_2^+ "paraexciton" which lies 12 meV lower. The limit of the yellow orthoexciton series occurs at 2.17 eV. The limit of the "green" (G) exciton series formed from the Γ_6^+ conduction band and the Γ_8^+ valence band occurs at 2.303 eV, and the limit of the "blue" (B) exciton series formed from the Γ_8^- conduction band and the Γ_7^+ valence band occurs at 2.624 eV. We use here the O_h cubic group notation $\Gamma_1, \Gamma_2^+, \Gamma_{12}^+, \Gamma_{25}^+, \Gamma_{15}$, which is equivalent o the notation $\Gamma_1, \Gamma_2, \Gamma_{12}, \Gamma_{25}', \Gamma_{15}'$ and the notation $\Gamma_1, \Gamma_2, \Gamma_3, \Gamma_4, \Gamma_5$, and which becomes in the double group $\Gamma_6^+, \Gamma_7^+, \Gamma_8^+, \Gamma_7^+ + \Gamma_8^+, \Gamma_6^+ + \Gamma_8^+$.

II. EXCITON THERMALIZATION BY ACOUSTIC-PHONON EMISSION

Figure 1 shows the band structure of Cu_2O at the zone center. The ground excitonic state, formed from the Γ_6^+ conduction band and Γ_7^+ valence band, is split into the ${}^1\Gamma_2^+$ paraexciton band and the ${}^3\Gamma_{25}^+$ orthoexciton band, which lies 12 meV higher by exchange interaction. In order to create excitons which can only thermalize by acoustic phonon emission, we have produced orthoexcitons resonantly via the phonon-assisted absorption process in which an exciton and a 13.8-meV Γ_{12}^- phonon are created simultaneously with absorption of a photon. This absorption process has been well studied in Cu_2O;[15] generation of orthoexcitons with emission of LO and other optic phonons also occurs, as well as phonon-assisted creation of paraexcitons with emission of a Γ_{25}^- optical phonon,[16] but the Γ_{12}^- phonon-assisted orthoexciton creation process has a factor of 30 greater oscillator strength than other phonon-assisted orthoexciton creation processes and a factor of 1500 greater strength than the phonon-assisted paraexciton creation process. Birman[17] has explained the greater strength of the Γ_{12}^--phonon-assisted process in the context of quadrupole-

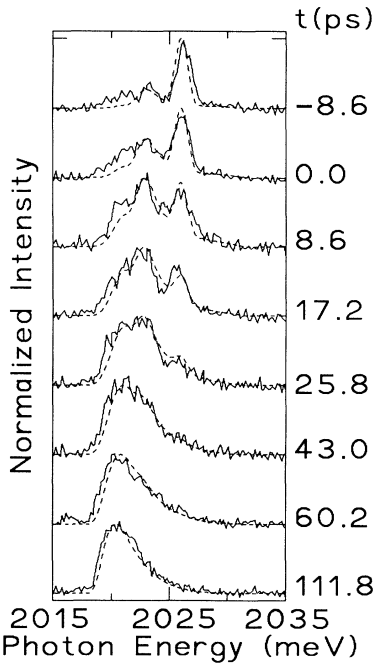

FIG. 2. Solid lines: the phonon-assisted luminescence of the orthoexcitons in Cu_2O at a lattice temperature of 16 K, at various delays after a synch-pumped dye laser pulse at photon energy 2.054 eV. The line shape gives the kinetic-energy distribution of the excitons directly. The excitons can only emit acoustic phonons to cool. Dashed lines: the prediction of the model of the energy distribution presented in the text. The entire series is fitted with variation of only one parameter, the deformation potential. The distribution at $t=111$ ps is within 5% of a Maxwell-Boltzmann distribution, $I(E) \propto E^{1/2} e^{-E/kT}$. The theory is convoluted with a triangle function of width 1.1 meV to account for the experimental spectral resolution. The laser generation function has the form $G(t) \propto e^{-(t/\gamma)^2}$, where $\gamma = 8$ ps.

dipole scattering theory by the fact that absorption with generation of the Γ_{12}^- phonon can involve the nearby Γ_8^- conduction state as an intermediate state, while all other phonons require the deeper Γ_{15}^- valence states as intermediate states.

Figure 2 shows the orthoexciton phonon-assisted luminescence spectrum at several delay times after a synch-pumped dye laser pulse hits a highly pure sample of Cu_2O in helium vapor. The time-resolved spectra were obtained with a Hamamatsu streak camera with 10–20-ps time resolution using a spectrometer grating of 1200 lines/mm. "$t=0$" is defined as the time of peak intensity of the laser pulse, or the half-maximum intensity of the total exciton luminescence. In this case the laser photons have energy 2.054 eV, which generate excitons 7 meV above the exciton band minimum energy of 2.033 eV by emission of the 13.8-meV Γ_{12}^- phonon, and appear in the Γ_{12}^--phonon-assisted luminescence at 2.026 eV. Since the generated excitons have only 7 meV kinetic energy, they cannot emit an optical phonon, because the lowest optical phonon energy is 11 meV (for the Γ_{25}^- phonon). The density of the excitons is low enough that exciton-exciton scattering does not play a role. In Sec. IV we discuss the exact density limit for the exciton-exciton scattering regime.

As time progresses, the excitons emit and absorb acoustic phonons until at late time they obtain a classical Maxwell-Boltzmann distribution given by $E^{1/2}\exp(-E/kT)$. The distribution at $t=111.8$ ps fits a Maxwell-Boltzmann law with $T=23$ K. At later times, the distribution maintains a Maxwell-Boltzmann shape but cools until it reaches the lattice temperature of 17 K.

The spectra in this figure have been fitted at all times to a numerical model using deformation potential theory. From the standard theory of acoustic-phonon emission for carriers via deformation potential interaction,[18] the matrix element for emission of a phonon with momentum $\hbar\mathbf{q}$ from an exciton state with momentum $\hbar\mathbf{k}$ to a state with momentum $\hbar(\mathbf{k}-\mathbf{q})$ is

$$|M_{\mathbf{k},\mathbf{q}}|^2=\frac{\hbar\Xi^2 q}{2\rho v V}(1\pm f_{\mathbf{k}-\mathbf{q}})(1+F_{\mathbf{q}})\ , \tag{1}$$

where the + sign applies for particles obeying Bose-Einstein statistics, such as excitons, and the − sign applies for those obeying Fermi-Dirac statistics, such as free carriers. Here Ξ is a deformation potential, i.e., an effective change in energy per unit strain $dE/d\varepsilon$, ρ is the crystal density, v the acoustic phonon speed, and V the crystal volume. $f_{\mathbf{k}}$ is the average occupation number for excitons with momentum $\hbar\mathbf{k}$ and $F_{\mathbf{q}}$ is the average occupation number for phonons with momentum $\hbar\mathbf{q}$. For absorption of a phonon with momentum $\hbar\mathbf{q}$ a factor $F_{\mathbf{q}}$ instead of $(1+F_{\mathbf{q}})$ is used.

The instantaneous change in the number of carriers with energy $E_{\mathbf{k}}$ due to phonon *emission* is therefore given by the Boltzmann equation

$$\frac{dn}{dt}(E_{\mathbf{k}})=\frac{dn_i}{dt}-\frac{dn_0}{dt}=\frac{2\pi}{\hbar}\frac{V}{(2\pi)^3}\int d^3q\,|M_{\mathbf{k}+\mathbf{q},\mathbf{q}}|^2 n(E_{\mathbf{k}+\mathbf{q}})\delta(E_{\mathbf{k}+\mathbf{q}}-E_{\mathbf{k}}-\hbar vq)$$
$$-\frac{2\pi}{\hbar}\frac{V}{(2\pi)^3}n(E_{\mathbf{k}})\int d^3q\,|M_{\mathbf{k},\mathbf{q}}|^2\delta(E_{\mathbf{k}}-E_{\mathbf{k}-\mathbf{q}}-\hbar vq)\ . \tag{2}$$

The rate of change due to phonon *absorption* can be calculated in a similar way. Here $n(E_{\mathbf{k}})=f_{\mathbf{k}}D(E_{\mathbf{k}})dE$. Integration over the angles can be eliminated from this equation analytically, so that the Boltzmann equation for phonon emission becomes

$$\frac{dn}{dt}(E_{\mathbf{k}})=\frac{1}{4\pi}\frac{\Xi^2 m}{\rho v\hbar^2}\left[\int dq\,\frac{q^2}{k}(1+F_q)n(E_k+\hbar vq)[1\pm f(E_k)]\Theta(E_{k+q}-E_k-\hbar vq)\Theta(E_k+\hbar vq-E_{k-q})\right.$$
$$\left.-\int dq\,\frac{q^2}{k}(1+F_q)n(E_k)[1\pm f(E_k-\hbar vq)]\Theta(E_{k+q}-E_k+\hbar vq)\Theta(E_k-\hbar vq-E_{k-q})\right]\ , \tag{3}$$

where $\Theta(E)$ is the Heaviside unit-step function. This form of the Boltzmann equation was used previously[19] to study the evolution of a Bose-Einstein gas toward condensation. To model the evolution of the gas, the kinetic-energy range of interest is broken into N channels, and the rates dn_0/dt and dn_i/dt for each channel for both phonon emission and absorption are calculated depending on the instantaneous value of n at each energy channel. After these rates are calculated for all energy channels, the distribution $n(E)$ is updated at each channel by adding $(dn_i/dt-dn_0/dt)dt$ to each channel for some small time step dt. The particles generated by the laser are added directly to $n(E)$ as $G(t)dt$, where $G(t)$ is a Gaussian distribution with a width obtained by a fit to the measured laser intensity versus time.

This model is therefore not a Monte Carlo method but rather a numerical solution of the exact Boltzmann equation. In Fig. 2 the dashed lines show the evolution of the distribution of excitons according to this model, assuming that the exciton density is low enough that the $(1\pm f)$ terms in the scattering matrix element are unimportant. The model reproduces the data quite well. Only one pa-

rameter is varied to fit the entire series of time-resolved spectra, which is the effective deformation potential Ξ. The fit to the data implies $\Xi = 1.8 \pm 0.03$ eV.

This number can be compared to the results of static stress experiments. The deformation Hamiltonian for the O_h point group is[20,21]

$$H_D = a\,\mathrm{Tr}\varepsilon - 3b\,[(L_z^2 - \tfrac{1}{3}L^2)\varepsilon_{zz} + \text{c.p.}] - 2d\sqrt{3}\,[\tfrac{1}{2}(L_yL_z + L_zL_y)\varepsilon_{yz} - \text{c.p.}]\,, \quad (4)$$

where ε_{ij} are components of the strain tensor, L_i are the angular momentum operators, and a, b, and d are deformation potentials in the notation of Pikus and Bir.[21] (The deformation potential a is defined positive for *decreasing* energy with compressive stress.) The terms denoted by c.p. are cyclic permutations. The deformation potential $a = dE/(dV/V)$ can be measured directly in hydrostatic-pressure experiments. Reimann and Syassen[22] report a value of -1.7 eV for the $n=1$ orthoexciton. While the band-gap deformation potential was measured as only -1.4 eV, the $n=1$ excitonic rydberg decreases due to the increase of the dielectric constant as the number of dipoles per unit volume increases. The total excitonic ground-state energy therefore increases faster than the band gap with increasing pressure.

The values of the shear deformation potentials b and d for the Γ_{25}^+ orthoexcitons can be deduced indirectly from uniaxial-stress experiments. Waters *et al.*[23] and Trebin, Cummins, and Birman[24] report values of b in the range -0.3 to -1.3 eV and d of the opposite sign and comparable magnitude, based on fits of uniaxial-stress data to perturbation solutions of the deformation Hamiltonian allowing mixing of the four "yellow" exciton states and eight "green" exciton states. The exact numbers depend sensitively on the values taken for the spin-orbit splitting of the yellow and green series and the electron-hole exchange energy. Apart from the theoretical fits, however, the uniaxial-stress data show that the contribution of the shear deformation potential is comparable to that of the hydrostatic term—the orthoexciton energy can shift either up *or* down with uniaxial stress by an amount comparable to the upward shift seen with hydrostatic stress, depending on the orthoexciton state.

To obtain the effective deformation potential for the orthoexcitons, the scattering rate, in other words, H_D^2, must be averaged over all possible strains $\varepsilon_{zz} = \varepsilon\cos^2\vartheta$ $\varepsilon_{yy} = \varepsilon\sin^2\varphi\sin^2\vartheta$, $\varepsilon_{xx} = \varepsilon\cos^2\varphi\cos^2\vartheta$, etc. The average of the square of the deformation potential in (4) is therefore

$$\begin{aligned}[\langle H_D\rangle^2]_\Theta &= [\langle 0|H_D|0\rangle^2]_\Theta + 2[\langle 0|H_D|1\rangle^2]_\Theta \\ &= a^2\varepsilon^2 + b^2\varepsilon^2[(-2\cos^2\vartheta + \sin^2\vartheta\cos^2\varphi + \sin^2\vartheta\sin^2\varphi)^2]_\Theta + 6d^2\varepsilon^2[\tfrac{1}{2}\cos^2\vartheta\sin^2\vartheta\sin^2\varphi + \tfrac{1}{2}\cos^2\vartheta\sin^2\vartheta\cos^2\varphi]_\Theta \\ &= (a^2 + \tfrac{4}{5}b^2 + \tfrac{2}{5}d^2)\varepsilon^2\,, \end{aligned} \quad (5)$$

where $[\ ]_\Theta$ indicates an average over all angles. For $a = -1.7 \pm 0.03$ eV from hydrostatic-pressure measurements, the effective deformation potential measured here, $\Xi = 1.8 \pm 0.03$ eV, implies $(b^2 + d^2/2)^{1/2} = 0.7 \pm 0.2$ eV. This compares to the values reported by Trebin, Cummins, and Birman[24] of $b \approx -d \approx -1.2$ eV from calculations based on uniaxial-stress data, which also yielded a high magnitude for the hydrostatic deformation potential, $a = -2.1$ eV. We note that the present method of time-resolved spectroscopy is a sensitive measurement of the excitonic deformation potential because the phonon emission rate depends on its square. Figure 3 shows the theoretical distribution at $t = 17.2$ ps under variation of the deformation potential.

The contribution of the shear deformation potential to the acoustic-phonon-emission rate raises the possibility of altering the energy loss rate of excitons by application of stress. This effect has been seen in Cu_2O for paraexcitons.[12] At high uniaxial stress the mixing of states yields a shear deformation potential for paraexcitons which is large and negative.[25] In Ref. 12 a significantly slower paraexciton cooling rate was seen at high stress than at zero stress. The contribution of shear stress to the LA phonon emission rate was not recognized at that time.

In the model presented here, the thermalization at early times does not depend sensitively on the value taken for the lattice temperature. Figure 3 shows the distribution at $t = 17.2$ ps for a lattice temperature of 10 K, 40% lower than the temperature used in the fit. To a first approximation, the change in lattice temperature only affects the broadening of the peaks. In the fit shown in Fig. 2, the lattice phonon temperature remains fixed at the value given by the Maxwell-Boltzmann distribution of the orthoexcitons at very late times, $t > 400$ ps. In other words, the phonon distribution is given at all times by the Planck distribution, $F(E) = 1/(e^{E/kT_L} - 1)$.

The other physical constants in the fit—the total exciton mass, the longitudinal acoustic (LA) phonon speed, and the crystal density—all have values from the literature. The crystal density is 6 g/cm^3, while the average longitudinal acoustic phonon velocity is taken as 4.5×10^5 cm/s.[26] The exciton mass of $(3.0 +/- 0.3)m_0$, from Yu and Shen[27] is confirmed in this experiment by the position of the first peak below the generated peak, which corresponds to single-acoustic phonon emission from the generated peak. The energy of this peak is given by $E_{\mathrm{gen}} - 2(2\ mv^2E_{\mathrm{gen}})^{1/2} - 2\ mv^2$, where E_{gen} is the generated exciton energy. In Ref. 27 this peak, labeled the "Y" peak, was interpreted as a resonant Raman line corresponding to emission of two Γ_{12}^- optical phonons and a longitudinal acoustic phonon. These studies show again the ambiguity of the differentiation between hot lumines-

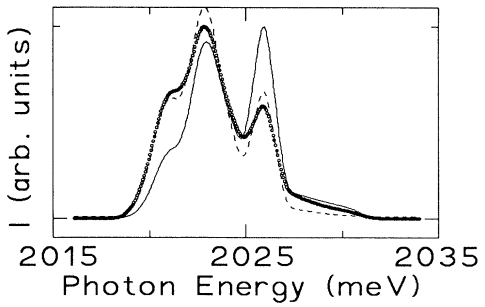

FIG. 3. The energy distribution predicted by the model discussed in the text under variation of two parameters. Dotted line: the prediction of the model used in the fit at $t=17.2$ ps in Fig. 2, with deformation potential $\Xi=1.8$ eV. Solid line: the prediction of the model with all parameters the same except $\Xi=1.4$ eV. Dashed line: the prediction of the model with all parameters the same ($\Xi=1.8$ eV) but lattice temperature $T_L=10$ K. At 60% lower temperature, the distribution at early times differs only in the broadening of the peaks.

cence and resonant Raman scattering. Here, the peak can clearly be seen as arising from a three-step process in which a real orthoexciton is generated by Γ_{12} phonon emission, loses energy by emission of a LA phonon, and then recombines via the Γ_{12}-phonon-assisted process. The height of this peak was enhanced relative to the rest of the luminescence in the experiments by Yu and Shen because of the short excitonic lifetime due to impurities in their sample. Indeed, in a later work,[28] Weiner and Yu pointed out that the "forbidden Raman" peaks in Cu_2O could be better explained as hot luminescence.

Transverse acoustic-phonon emission does not play a significant role in the cooling of the excitons at this temperature. From the relative height of the LA and TA emission peaks in the study by Yu and Shen,[27] it is known that emission of TA phonons by orthoexcitons occurs at a rate 50 times lower. We therefore do not include TA emission in the numerical model presented here.

The solution method of the model here is quite general. Figure 4 shows a hypothetical case in which particles with the same mass as the excitons in Cu_2O are created at the same kinetic energy and relax via acoustic-phonon emission with the same crystal constants, but obey Fermi-Dirac statistics-like free carriers. The generated distribution is broader here than in the model of Fig. 2 because Pauli exclusion saturates the laser absorption at the center of the energy distribution. Carrier-carrier interactions are ignored here, so this case corresponds to the low-density limit for free carriers in a semiconductor. The cooling process is much slower due to the Pauli exclusion of states, and at late times the distribution takes on the familiar Fermi cutoff, in this case at roughly 5 meV for a density of $5\times10^{18}/\text{cm}^3$.

Figure 5 shows another hypothetical case in which the excitons in Cu_2O are given a density above the critical

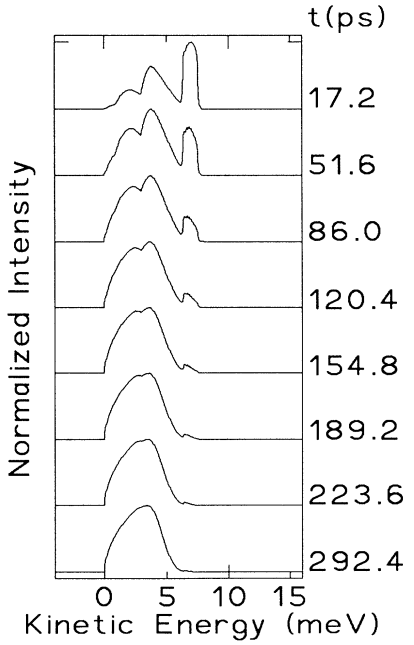

FIG. 4. A solution of the kinetic model discussed in the text for a hypothetical case of fermion thermalization (twofold spin degeneracy). The carriers in this case have mass $m=3m_0$, density $5\times10^{18}/\text{cm}^3$, and exist in a lattice with acoustic-phonon speed 4.5×10^5 cm/s and deformation potential 1.8 eV. Lattice temperature is $T_L=2$ K. At late times the distribution reaches the Fermi distribution $I(E)\propto E^{1/2}/(e^{(E-\mu)/kT_L}+1)$.

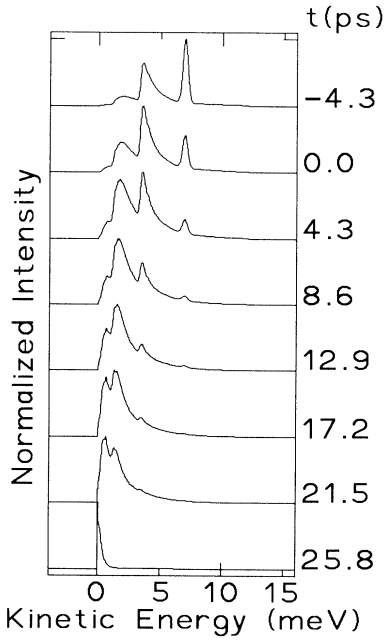

FIG. 5. A solution of the kinetic model discussed in the text for a hypothetical case of boson thermalization (threefold spin degeneracy). This case corresponds to the case of excitons in Cu_2O at density $10^{18}/\text{cm}^3$ and lattice temperature 16 K with carrier-carrier interactions "turned off." A sudden transition to Bose-Einstein condensation is seen at $t\sim25$ ps.

density for Bose-Einstein condensation at the lattice temperature. The excitons quickly emit a series of phonons, and exhibit a sharp onset of Bose-Einstein condensation at $t=25$ ps. This model is unphysical for Cu_2O, however, because it neglects exciton-exciton interactions, and at the densities necessary for Bose-Einstein condensation, exciton-exciton interactions cannot be ignored, as discussed in Sec. IV. A two-exciton Auger process[11,12] which results in annihilation of one exciton has been shown to be an important source of heating of a dense exciton gas in Cu_2O.[8] Elastic collisions between excitons can also broaden the excitonic kinetic-energy distribution.

III. EXCITON THERMALIZATION BY OPTICAL-PHONON EMISSION

By tuning the laser to higher frequencies we can generate orthoexcitons in a regime where they can emit both acoustic phonons and optic phonons.

Figure 6 shows a series of time-resolved spectra as in Fig. 2, with laser photon energy 2.067 eV, generating orthoexcitons with kinetic energy of 20 meV which appear in the Γ_{12} phonon assisted luminescence at 2.039 eV.

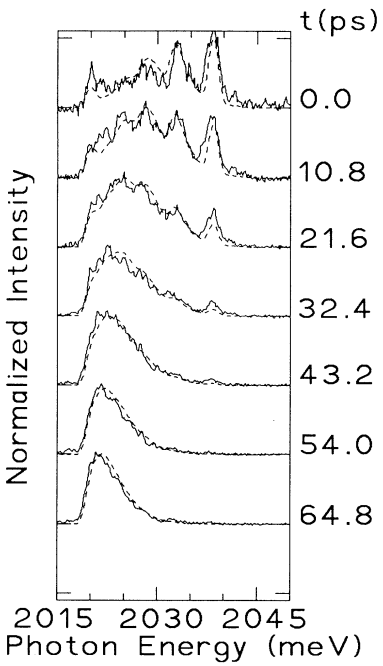

FIG. 6. Solid lines: the phonon-assisted luminescence of orthoexcitons in Cu_2O at a lattice temperature of 18 K, at various delays after a synch-pumped dye laser pulse at photon energy 2.067 eV. The excitons can emit three optical phonons as well as acoustic phonons at this generation energy. Dashed line: the prediction of the model discussed in the text with the same deformation potential for acoustic phonon emission as used in Fig. 2 The optical-phonon deformation potential is fixed by this fit, because the overall cooling rate of the excitons at early time depends not only on the acoustic-phonon-emission rate, but also the optical-phonon-emission rate. The laser generation function has the form $G(t)\propto e^{-(t/\gamma)^2}$, where $\gamma=25$ ps.

The generated orthoexcitons can emit three kinds of optical phonons—the 11-meV Γ_{25}^- phonon, the 13.8-meV Γ_{12}^- phonon, and the 18.7-meV Γ_{15}^- phonon (there are actually two Γ_{15}^- TO modes and a Γ_{15}^- LO mode lying 0.5 meV higher).

The spectra in this figure are fit to a model like that discussed above for acoustic-phonon emission but also including optic phonon emission by a nonpolar optical-phonon deformation potential. Excitons in Cu_2O are not expected to have a strong Fröhlich interaction because the LO and TO modes are very close in energy, leading to a weak frequency dependence of the dielectric constant, and because the electron and hole masses are nearly equal.[29] The standard theory for nonpolar optic phonon emission[17] gives the matrix element as

$$|M_{\mathbf{k},\mathbf{q}}|^2=\frac{\hbar^2D^2}{2\rho E_0 V}(1\pm f_{\mathbf{k}-\mathbf{q}})(1+F_{\mathbf{q}})\ , \tag{6}$$

where D is the optical deformation potential in units of eV/cm, and E_0 is the energy of the optical phonon. For an allowed process with constant phonon frequency the matrix element is independent of $\mathbf{q}$. In fact, all of the single optical-phonon emission processes are forbidden by parity in Cu_2O at $\mathbf{q}=0$, because the phonons have negative parity and the orthoexciton (and paraexciton) positive. The matrix element should therefore be proportional to q. Since the optical phonons emitted by the excitons all have momentum about equal to $(2mE_0)^{1/2}$, however, we assume no $\mathbf{q}$ dependence and use an average value of D. An exact Boltzmann equation can be written and solved numerically for this matrix element just as discussed in Sec. II.

Each of the optic phonons can have a separate deformation potential. The ratios of these deformation potentials can be set by comparison with the data of Yu and Shen[27] for the relative efficiency of the three "three-phonon Raman lines." The heights of these lines, which are simply due to hot luminescence following emission of an optical phonon by a real exciton, are proportional to the square of the nonpolar optical deformation potentials involved, divided by the phonon energy. In the data of Ref. 27, the Γ_{15}^- phonon emission line, which corresponds to the sum of the contributions of two TO modes and the LO mode, has a maximum intensity about three times higher than the two lower-energy phonon lines, which are roughly equal in maximum efficiency. The deformation potentials of these phonons are therefore fixed at (0.72 ± 0.08) times the Γ_{15}^- deformation potential.

Four lines are visible below the generated peak at early times. The first peak, which appears 5 meV below the generated distribution, corresponds to single acoustic-phonon emission. Three lines occur at lower energies due to the three optical phonon energies allowed in emission. At late times, the distribution takes on the Maxwell-Boltzmann distribution via acoustic-phonon emission and absorption.

In fitting this high-kinetic-energy data, we have taken into account the fact that the long-wavelength approximation breaks down at high acoustic-phonon frequency.

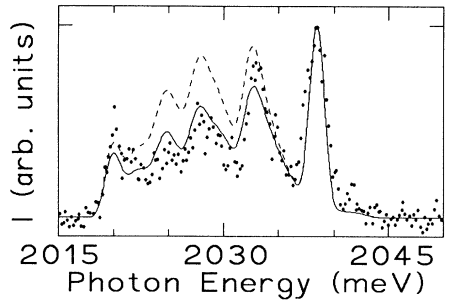

FIG. 7. Solid circles: the data of Fig. 6 at $t=0$. Solid line: the model calculation for the distribution at $t=0$ shown in Fig. 6, which includes the correction term $(1+a_0^2q^2/16)^{-2}$ in the acoustic-phonon-scattering matrix element. Dashed line: the same calculation, with the same acoustic- and optical-phonon deformation potentials, but without the high-q correction to the acoustic-phonon-scattering matrix element.

For an exciton with equal hole and electron masses, the band-gap deformation potential must be corrected to become[30]

$$\Xi' = \Xi(1+a_0^2q^2/16)^{-2} , \tag{7}$$

where a_0 is the excitonic Bohr radius (=7 Å in Cu_2O) and q is the magnitude of the phonon wave vector. This correction is significant at the initial excitonic energies in this case. Figure 7 shows the energy distribution at $t=0$ and a fit of the model with and without the high-q correction factor. If the correction factor is neglected, then assuming the same deformation potential as deduced in the low-kinetic-energy case, 1.8 eV, gives too fast a cooling rate even if the optic phonon emission rate is set to zero.

Using the value for Ξ from the fit in the acoustic-phonon-emission regime, then, and the known value for the excitonic Bohr radius in the short-wavelength correction factor, we fit the entire time series of Fig. 6 by variation of a single parameter, the Γ_{15}^- optical-phonon deformation potential. From the fit to the data, the average optical deformation potential for the Γ_{15}^- phonons is estimated as $(1.7\pm0.2)\times10^7$ eV/cm$=0.17\pm0.02$ eV per angstrom of atomic displacement. This corresponds to an optical-phonon emission time of roughly 30 ps, which is quite long compared to semiconductors such as GaAs with allowed polar-optic-phonon emission times of 180 fs. This can be understood in part because the single-optic-phonon emission processes are all forbidden by symmetry, as mentioned above.

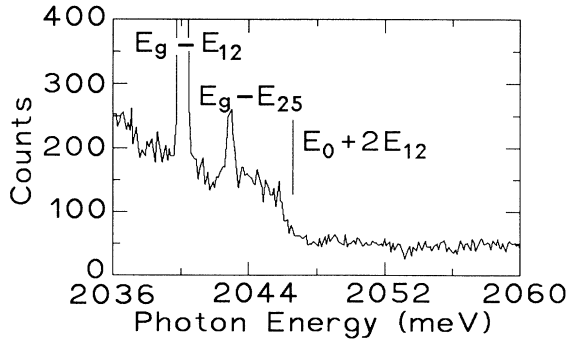

FIG. 8. The luminescence spectrum of orthoexcitons in Cu_2O under cw excitation at laser photon energy 2.068 eV. The two sharp lines labeled $E_g - E_{12}$ and $E_g - E_{25}$ are the hot luminescence peaks due to generation of excitons via Γ_{12}^- and Γ_{25}^- optical phonon emission, respectively. The sharp "ledge" at exciton kinetic energy $2E_{12}$ arises due to the allowed two-phonon emission process at this energy.

At higher energy, excitons may lose energy in a parity-conserving process by emitting two optic phonons simultaneously. This would allow a much faster emission rate. Figure 8 shows the orthoexciton luminescence in the range 2.036–2.060 eV during cw laser excitation at photon energy of 2.068 eV. The luminescence fits a Maxwell-Boltzmann distribution at low energy. The "ledge" in the luminescence at 2.046×6 eV corresponds to exciton kinetic energy of 27.6 meV, or the energy at which excitons can emit two 13.8-eV optic phonons. Interestingly, no similar ledge is seen for the two-Γ_{25}^--phonon process at 22-meV excitonic kinetic energy (2.041-eV photon energy), although this process is also parity allowed.

Since we can assume that the scattering rate of excitons *into* states with energy on either side of the ledge is the same, the difference in exciton population on the two sides of the ledge may be due to the increased rate out of states which can emit two Γ_{12}^- phonons. By the ratio of luminescence intensity of the two sides of the ledge, we can estimate that the two-phonon emission process would be at least ten times faster than the sum of all single-phonon emission processes at that energy. We can only put a bound on this ratio because the lower side of the ledge is essentially just the dark count of the photomultiplier detector. Mysyrowicz, Hulin, and Hanamura[31] report a formation time of only 250 fs for $n=1$ excitons after band-to-band generation of free carriers in Cu_2O. Assuming that exciton formation from free carriers also occurs via the allowed two-phonon emission process, this places an upper bound on the time per two-phonon emission of 250 fs, which is not inconsistent with our measurements.

Figure 9 summarizes all of the phonon-emission data. The solid line shows the total energy loss rate per exciton versus the temperature of the excitons, assuming that the excitons have a Maxwell-Boltzmann distribution, for the measured phonon-emission rates (the two-Γ_{12}^--phonon-emission process is given a rate ten times faster than the Γ_{15}^- emission process.) At very low temperature, the effects of suppressed LA phonon emission, reported by Trauernicht *et al.*[3] based on measurements of the diffusion constant, are included. As seen in this figure, the energy loss rate deviates substantially from the $T^{3/2}$ power law derived in the high-temperature limit[32] even at temperatures as high as 20 K. At temperatures above 30 K, optical-phonon emission from high-kinetic-energy excitons contributes an increasing amount to the cooling rate. The dashed-dotted line shows the energy loss rate when the fast two-phonon process for excitons with $E>27.6$ meV is not included; the dashed line at high

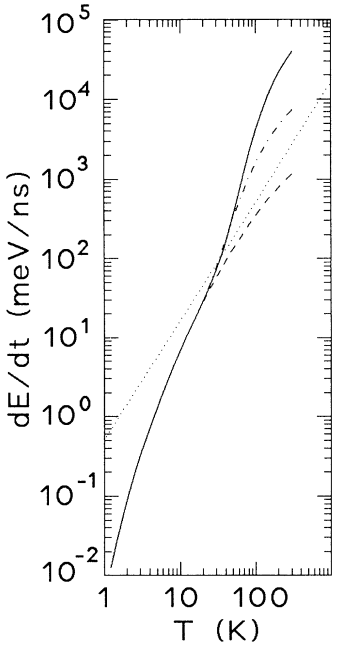

FIG. 9. Solid line: the energy-loss rate per exciton in Cu_2O as a function of temperature, assuming the excitons have a Maxwell-Boltzmann distribution and the lattice temperature is insignificant compared to the excitonic temperature, based on the measurements of phonon emission rates reported in this paper. Dotted-dashed line: the energy-loss rate if the two-phonon emission process for $E > 27.6$ meV is not included. Dashed line: the energy-loss rate if only acoustic-phonon emission is included with the high-q correction term discussed in the text. Dotted line: the high-energy acoustic-phonon energy loss rate for the same deformation potential assuming a $T^{3/2}$ power law. This power law fails at low temperature because not all excitons can emit LA phonons, as reported in Ref. 3, and at high temperature because of the breakdown of the long-wavelength approximation, as discussed in the text.

temperature shows the contribution of acoustic phonons alone, including the high-q correction factor (8).

The energy loss rate in the range 8–30 K is consistent with that reported in Ref. 8, approximately 0.2 meV/ns $K^{3/2}$. Reference 8 reported a lower value of the deformation potential for acoustic-phonon emission, however, because the effect of suppressed LA phonon emission at low temperature, which causes a deviation from the $T^{3/2}$ power law, was not included in fitting the data.

IV. EXCITON-EXCITON SCATTERING

So far, we have considered only inelastic scattering processes for the excitons, namely, phonon emission. Excitons can also scatter off each other. What is the effect of carrier-carrier interactions?

Little is known about the exciton-exciton scattering process. Hanamura and Haug[33] generalized the solution for interaction between two hydrogen atoms to apply to the case of a heavy-hole exciton. In that case, an effective hard-core radius of about two times the Bohr radius is obtained. The effects of light mass and Pauli exclusion were not included in that model, however. In a different approach, Bassani[34] calculated the binding energy of the biexciton in Cu_2O and predicted that no biexcitons exist, which leads to the prediction that all exciton-exciton interactions are repulsive. Bobrysheva and Moskalenko[35] later modified that approach to predict that orthoexcitons with summed spin $S=1$ could form a biexciton with binding energy 0.7 meV. No evidence for the existence of biexcitons has been reported in Cu_2O.

An elastic exciton-exciton scattering process will not change the rate of energy loss of the excitons. Interparticle scattering will show up in the time-resolved spectra as a washing out of the sharp features seen in the data of Secs. II and III. Reference 17 used a Boltzmann equation similar to Eq. (2) to simulate the effect of elastic exciton-exciton scattering on the kinetic energy distribution. Washing out of sharp features was shown to occur on time scales of the order of twice the average time for an exciton-exciton collision; in other words, sharp peaks due to phonon emission will disappear when the average collision time is comparable to the time for phonon emission and absorption.

The fact that we see sharp features in the excitonic kinetic-energy spectrum allows us to place an upper bound on the range of elastic exciton-exciton scattering by knowing the density of excitons during the observations. In these experiments, the initial exciton density was varied up a maximum of approximately $3\times10^{16}/cm^3$. This corresponds to a laser pulse energy of 9×10^{-10} J, a focal spot size of 20 μm inside the crystal, and an absorption length of the laser light at 6000 Å measured to be roughly 200 μm. As laser power was varied by more than an order of magnitude, no appreciable change was observed in the time-resolved spectra such as those shown above; in particular, the early time peaks were not "washed out" at the highest density.

This places a limit on the possible interaction cross section of the excitons. To estimate the scattering cross section we use the classical rate formula for hard spheres:

$$\tau=\frac{1}{n\sigma v}\ , \tag{8}$$

where n is the density, v is the average velocity, and σ is the scattering cross section. For an average energy of 40 K at early times, corresponding to an average velocity of 2.5×10^6 cm/s, a scattering time τ of greater than 40 ps (the time scale of the sharp phonon-emission peaks we see) at a density of $3\times10^{16}/cm^3$ implies an exciton-exciton scattering cross section of at most 3000 $Å^2$, or a hard-core scattering radius of at most 30 Å, which is four times the excitonic Bohr radius of 7 Å. This upper bound is not surprising given the fact that excitons are expected to be weakly interacting with a hard-core radius of two or three excitonic Bohr radii.

V. CONCLUSIONS

We have shown that the statistics of excitons far from equilibrium can be well modeled by a solution of an exact

Boltzmann equation for phonon emission and absorption, using deformation potential theory. This method of solution has the advantage that the carrier distribution need not be assumed to have a Maxwell-Boltzmann or a Fermi-Dirac distribution at every point in time, but rather evolves the distribution *toward* an equilibrium distribution.

The deformation potential for longitudinal acoustic-phonon emission by excitons in Cu_2O is measured here as 1.8 ± 0.03 eV. The deformation potential for nonpolar optic-phonon emission is measured as $(1.7\pm0.2)\times10^7$ eV/cm for the lowest-energy TO and LO phonons. This yields a rather slow optical-phonon emission rate at low-exciton kinetic energies, roughly $\frac{1}{30}$ ps^{-1}. In fact, the rate of optical-phonon emission is comparable to the rate of acoustic-phonon emission at the same energies. This can be understood as due to the fact that optical-phonon emission is forbidden for excitons by parity conservation at the zone center. We see evidence for a two-phonon emission process which conserves parity with a rate on the order of $\frac{1}{300}$ fs^{-1}.

The value for the acoustic-phonon deformation potential deduced here is in essential agreement with measurements of the shift of the orthoexciton energy with hydrostatic and uniaxial pressure. The contribution of shear stress terms in the deformation potential is small, but discernible given the relatively small error in our estimate of the acoustic-phonon-phonon scattering rate. A correction for the breakdown of the long-wavelength approximation in the acoustic-phonon scattering matrix element is necessary to fit the data at high-initial excitonic kinetic energy. This correction factor depends only on the excitonic rydberg, to first order. Using the expected value of the excitonic Bohr radius, 7 Å, gives a correction which fits the data perfectly.

The energy loss rate for excitons in Cu_2O never follows a $T^{3/2}$ law. At temperatures below 20 K, the energy loss rate is slower than expected from textbook deformation potential theory because of the inhibition of acoustic-phonon emission for excitons in low-energy states. At higher temperatures, optical-phonon emission becomes significant. Therefore the overall power law for the energy loss rate as a function of temperature in Cu_2O is close to T^3 in the range 1–200 K.

Our measurements put a rough upper bound on the hard-core scattering radius of excitons in Cu_2O of approximately four excitonic Bohr radii, or 30 Å. Therefore the excitons can be considered as weakly interacting up to very high densities.

ACKNOWLEDGMENTS

W. Rühle was instrumental in the initial stages of these experiments and we thank him for allowing us to use the picosecond laser and detection system in these experiments. We thank D. Mowbray for assistance in taking the data of Fig. 8. We thank J. P. Wolfe for kindly lending us the high-purity natural samples of Cu_2O originally obtained as a gift from P. J. Dunn of the Smithsonian Institute. One of us (D.S.) is indebted to the Alexander von Humboldt Society for financial support and to the Max-Planck-Institute für Festkörperforschung for its hospitality.

[1]For a review of the properties of Cu_2O, see V. T. Agekyan, Phys. Status Solidi A **43**, 11 (1977).

[2]A. Mysyrowicz, D. Hulin, and A. Antonetti, Phys. Rev. Lett. **43**, 1123 (1979); **43**, 1275(E) (1979).

[3]D. P. Trauernicht, J. P. Wolfe, and A. Mysyrowicz, Phys. Rev. Lett. **52**, 855 (1984); D. P. Trauernicht and J. P. Wolfe, Phys. Rev. Lett. B **33**, 8506 (1986).

[4]D. Hulin, A. Mysyrowicz, and C. Benoit a la Guillaume, Phys. Rev. Lett. **45**, 1970 (1980).

[5]D. Snoke, J. P. Wolfe, and A. Mysyrowicz, Phys. Rev. Lett. **59**, 827 (1987).

[6]D. W. Snoke, J. P. Wolfe, and A. Mysyrowicz, Phys. Rev. Lett. **64**, 2543 (1990).

[7]D. W. Snoke, J. P. Wolfe, and A. Mysyrowicz, Phys. Rev. B **41**, 11 171 (1990).

[8]D. W. Snoke and J. P. Wolfe, Phys. Rev. B **42**, 7876 (1990).

[9]D. W. Snoke. J.-L. Ling, and J. P. Wolfe, Phys. Rev. B **43**, 1226 (1991).

[10]V. B. Timofeev, V. D. Kulakovskii, and I. V. Kukushkin, Physica B+C **117/118**, 327 (1983).

[11]A. Mysyrowicz, D. Hulin, and C. Benoit a la Guillaume, J. Lumin. **24/25**, 629 (1981).

[12]D. P. Trauernicht, A. Mysyrowicz, and J. P. Wolfe, Phys. Rev. B **34**, 2561 (1986).

[13]As seen, for example, in liquid helium-4 even above T_c. See G. D. Mahan, *Many-Particle Physics* (Plenum, New York, 1981), p. 883.

[14]For a review of fast thermalization processes of carriers in semiconductors like GaAs, see *Semiconductors Probed by Ultrafast Laser Spectroscopy,* edited by R. R. Alfano (Academic, Orlando, 1984), Vol. I.

[15]I. Pastyrnak, Phys. Status Solidi **1**, 888 (1959); J. B. Grun, M. Sieskind, and S. Nikitine, J. Phys. Chem. Sol. **19**, 189 (1961).

[16]P. D. Bloch and C. Schwab, Phys. Rev. Lett. **41**, 514 (1978).

[17]J. L. Birman, Solid State Commun. **13**, 1189 (1973).

[18]K. Seeger, *Semiconductor Physics* (Springer-Verlag, New York, 1973), Chap. 6.

[19]D. W. Snoke and J. P. Wolfe, Phys. Rev. B **39**, 4030 (1989).

[20]M. Cardona, *Modulation Spectroscopy,* Solid State Physics, Supp. 11 (Academic, New York, 1969).

[21]G. E. Pikus and G. L. Bir, Fiz. Tverd. Tela (Leningrad) **1**, 1642 (1959) [Sov. Phys. Solid State **1**, 1502 (1959)].

[22]K. Reimann and K. Syassen, Phys. Rev. B **39**, 11113 (1989).

[23]R. G. Waters, F. H. Pollak, R. H. Bruce, and H. Z. Cummins, Phys. Rev. B **21**, 1665 (1980).

[24]H.-R. Trebin, H. Z. Cummins, and J. L. Birman, Phys. Rev. B **23**, 597 (1970).

[25]A. Mysyrowicz, D. P. Trauernicht, J. P. Wolfe, and H.-R. Trebin, Phys. Rev. B **27**, 2562 (1983).

[26]J. Berger, J. Castiang, and M. Fischer, J. Phys. (Paris) **40**, Supp. 11, 13 (1979); J. Hallberg and R. C. Hanson, Phys. Status Solidi **42**, 305 (1970).

[27]P. Y. Yu and Y. R. Shen, Phys. Rev. Lett. **32**, 939 (1974); Phys. Rev. B **12**, 1377 (1975).

[28]J. S. Weiner and P. Y. Yu, Solid State Commun. **50**, 493 (1984).

[29]A. Goltzene and C. Schwab, in Solid State Commun. **18**, 1565 (1976), give m_e as $0.98m_0$, and J. H. Hodby, T. G. Jenkins, C. Schwab, H. Tamura, and D. Trivich, in J. Phys. C **9**, 1429 (1976), give m_h as $0.7m_0$. The total excitonic mass $M=m_e+m_h=1.7m_0$ does not agree with that reported here and in Ref. 27, $M=3m_0$, possibly due to k-dependent terms in the spin-exchange energy of the orthoexciton.

[30]M. Cardona, *Light Scattering in Solids* (Springer-Verlag, Berlin, 1982), Vol. 11, pp. 129–138.

[31]A. Mysyrowicz, D. Hulin, and E. Hanamura, in *Ultrafast Phenomena VII,* edited by C. B. Harris, E. P. Ippen, G. A. Moirou, and A. H. Zewail (Springer-Verlag, Berlin, 1990), p. 244.

[32]See, for example, E. M. Conwell, Solid State Physics (Academic, New York, 1967), Suppl. 9, p. 122.

[33]E. Hanamura and H. Haug, Phys. Rep. **33**, 209 (1977).

[34]F. Bassani and M. Rovere, Solid State Commun. **19**, 887 (1976).

[35]A. I. Bobrysheva and S. A. Moskalenko, Phys. Status Solidi A **43**, 11 (1977).